Al 3p electronic distributions in AlMn crystalline, quasicrystalline and amorphous alloys

1991 J. Phys.: Condens. Matter 3 2157

(http://iopscience.iop.org/0953-8984/3/13/018)

J. Phys.: Condens. Matter 3 (1991) 2157–2166. Printed in the UK

Al 3p electronic distributions in AlMn crystalline, quasicrystalline and amorphous alloys

Esther Belin† and Agnès Traverse‡

† Laboratoire de Chimie Physique (UA176), Université Pierre et Marie Curie, 11 rue Pierre et Marie Curie, 75231 Paris Cédex 05, France

‡ Centre de Spectrométrie Nucléaire et Spectrométrie de Masse, Bâtiment 108, 91405 Campus d'Orsay, France

Received 26 October 1990, in final form 9 January 1991

Abstract. Al $K\beta$ soft x-ray emission spectra (p states of the valence band $\rightarrow$ 1s) have been analysed for several $Al_{100-x}Mn_x$ alloys of different structural arrangements and compositions and compared with pure Al. Differences are observed according to the structural state of the sample; the states near the Fermi level appear to be long-range order-dependent while those at $E_F + 6.5$ eV are sensitive to a shorter-range order. A partial p DOS at E_F is related to both the Mn concentration and the structural state; this is in line with resistivity measurements on similar alloys.

1. Introduction

Since the discovery in 1984 of quasicrystalline phases in Al–Mn alloys (Shechtman *et al* 1984), much attention has been devoted to problems related to the feasibility of these materials (Shechtman 1988, Harmelin 1988) and also to their structural determination both theoretically (Gratias 1989, Bendersky *et al* 1989, Kléman 1990) and experimentally by transmission electron microscopy, EXAFS and x-ray or neutron diffraction measurements (Harmelin 1988, Sadoc and Dubois 1989, Denoyer *et al* 1990, Ingersent and Steinhart 1990, Proceedings of the LAM 7 Conference 1990, Bellissent *et al* 1987). Investigations have also been made into the electronic properties of these materials (Choy 1985, Berger *et al* 1986, McHenry *et al* 1986, Bahadur *et al* 1987, Smith and Ashcroft 1987, Friedel 1988, Mayou *et al* 1988, Ederer *et al* 1988, Fujiwara 1989).

Soft x-ray spectroscopy (SXS) allows us to investigate the electronic structure of solids. Indeed, x-ray emission and photoabsorption processes involve an atomic inner level of a given angular momentum and states of the valence or conduction bands; as the x-ray transitions are governed by dipole selection rules, partial local occupied or empty electronic distributions around an atom in a solid can be achieved separately. With this technique, effects of allotropy and disorder on the electronic distributions of solids have been evidenced for several kinds of materials (see for example Guita *et al* 1986, Belin *et al* 1987, Belin *et al* 1988).

From a previous series of experiments, performed by SXS measurements on $Al_{84}Mn_{16}$ and $Al_{80}Mn_{20}$ samples prepared by ion beam mixing of Al/Mn multilayers, we concluded that the Al 3p occupied and empty distributions show differences according to the atomic structure of the sample: crystalline, amorphous or quasicrystalline (Traverse *et al* 1988).

0953-8984/91/132157 + 10 $03.50

Table 1. Structural state and preparation techniques of our different $Al_{100-x}Mn_x$ alloys.

% Mn atoms	Structural state	Ion beam mixing	Rapid solidification
14	C	*	*(1)
	I		*(1, 3)
16	C	*	
	I	*	
20	T		*(2)
21	C (αAlMnSi)		*(1)
	I (AlMnSi)		*(1)
	A	*	
22	T		*(1)

We have extended these experiments to other $Al_{100-x}Mn_x$ alloys of different nominal concentrations prepared by either ion beam mixing or rapid solidification techniques.

In this paper we report on the Al 3p valence distributions which we obtained from x-ray Al Kβ emission (valence band$\rightarrow$ 1s) for a series of $Al_{100-x}Mn_x$ alloys, and we focus on both the effects of atomic structure and of Mn concentration.

The paper is organized as follows: in the first part, we describe the experimental procedure; in the second one, we present the results and we discuss them in the last section.

2. Experimental procedure

The Al Kβ x-ray spectra were created using a Johann type vacuum spectrometer equipped with a $10\bar{1}0$ quartz crystal bent to a radius of 50 cm, and a proportional flow A-CH_4 counter whose entrance slit was set on the focusing cylinder. Convenient statistical count accuracy was achieved by recording the spectra along the focusing cylinder with successive scans of steps 0.16 eV wide. In the energy range of the Al Kβ emission (1545–1553 eV) the experimental resolution is about 0.2 eV.

The samples were either thin films prepared by ion beam mixing or small pieces of ribbon prepared by rapid solidification. They were stuck with ultra vacuum grease or silver dag onto suitable metallic water-cooled holders which were used as anodes of the x-ray tube and were irradiated by incoming electrons of energy 3000 eV.

Several different $Al_{100-x}Mn_x$ alloys were analysed: crystalline (C), icosahedral (I), decagonal (T) and amorphous (A) (table 1) whose structural states have been controlled by either x-ray diffraction, electronic diffraction or transmission electron microscopy. All of them were single phased except the I-$Al_{86}Mn_{14}$ in which a faint Al contamination remained (about 5%). Results concerning two-phased samples are also reported.

3. Results

As already mentioned, the Al 3p distribution results from transitions of a valence electron to the Al 1s level. To compare the distributions obtained for the different samples, it is necessary to adjust the corresponding spectra to the same energy scale.

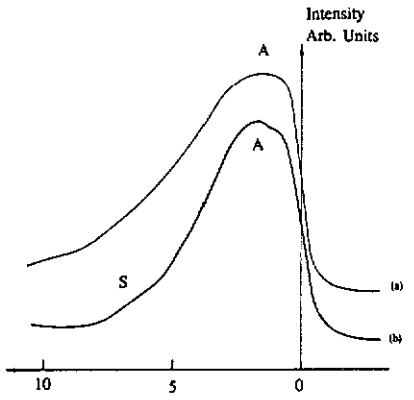

Figure 1. Al 3p distribution curves in pure Al, curve (a) and in crystalline Al_6Mn, curve (b).

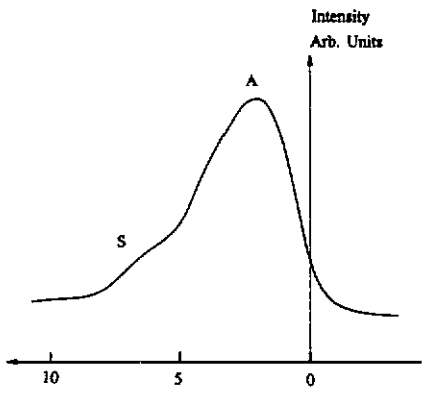

Figure 2. The Al 3p distribution curve in amorphous $Al_{79}Mn_{21}$.

This is achieved by taking the Fermi level as the origin of the energies which we locate on the x-ray transition energy scale from the value of the Al 1s energy level. To obtain this value, two different measurements are necessary: first, from SXS experiments, we determine the energy of the x-ray transition Al Kα: $2p_{3/2} \rightarrow 1s$; second, from XPS experiments, we measure the binding energy of the core Al $2p_{3/2}$ level which is referred to the Fermi level. The combination of those measurements leads to an uncertainty of ± 0.2 eV on the position of E_F.

We have found (Traverse *et al* 1988) that the Fermi level energy positions of all the C and I samples prepared by the ion beam mixing technique are the same within experimental uncertainty. We assumed this to be true for all the $Al_{100-x}Mn_x$ alloys that we have investigated, whatever their preparation technique. Notice that, contrary to our results, from a calculation performed in a cluster model, McHenry *et al* (1986) found a 0.9 eV shift of the position of E_F towards low binding energies when going from crystalline to icosahedral Al–Mn.

Our curves are presented with E_F as origin of the binding energy (BE) scale; they are normalized between the maximum and the intensity value at about 3 eV beyond E_F, that is to say in a range where the intensity variation is negligible.

Figure 1 shows the Al 3p distributions in pure Al and in crystalline $Al_{86}Mn_{14}$. The curve for pure Al (figure 1(*a*)) exhibits the well known arctangent shape near the Fermi level and a band tail towards high BE; its full width at half maximum (FWHM) is 5.3 ± 0.1 eV in agreement with previous measurements (Sénémaud 1966). The width of the Al 3p distribution in $Al_{86}Mn_{14}$ (figure 1(*b*)) is reduced so that the FWHM becomes 4.2 ± 0.1 eV. The edge retains the arctangent shape and is abrupt as in pure metal; within experimental uncertainty, it cuts the Fermi level at about half maximum. The top of the band, A, is split into two parts at 1.7 and 0.8 ± 0.1 eV, respectively, the separation occurs at $+1.45 \pm 0.1$ eV. A slight shoulder, denoted S, is also noticeable in the range of about +6.5 eV. Whatever their preparation technique, the $Al_{86}Mn_{14}$ samples displayed the same Al Kβ curve except in the range of shoulder S. We will discuss this point later.

Figure 2 shows the curve for the Al 3p distribution in A-$Al_{79}Mn_{21}$. The edge is slightly less abrupt and at half maximum its distance with respect to E_F is about +0.4 eV. Peak A is situated at $+2.0 \pm 0.1$ eV, it is no longer split into two parts, and its shape is rounded. On the high binding-energy side structure S is also observed. The FWHM of the band is 4.2 ± 0.1 eV. The intensity at E_F is 27% that of the maximum.

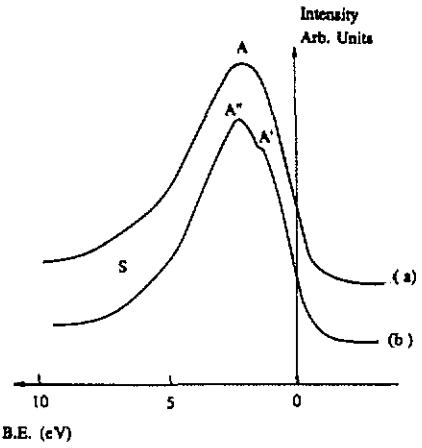

Figure 3. Al 3p distribution curves in quasicrystalline $Al_{100-x}Mn_x$ alloys: icosahedral $Al_{79}Mn_{21}$, curve (a) and decagonal $Al_{78}Mn_{22}$, curve (b).

The curve of figure 3(*a*) corresponds to the I-$Al_{79}Mn_{21}$ phase. Its shape is very similar to that of the amorphous sample: peak A, rather rounded, is at $+2.0 \pm 0.1$ eV, structure S is noticeable, and the FWHM is 4.3 ± 0.1 eV. However, the edge is slightly less abrupt than in the A phase; at half maximum it is at about +0.25 eV and the intensity at E_F is about 34% that of the maximum. Notice that the FWHM of I-$Al_{86}Mn_{14}$, once corrected for the slight Al contamination, is 4.5 ± 0.1 eV. Peak A is at $+1.8 \pm 0.1$ eV and the intensity at E_F is 42% that of the maximum.

The curve of figure 3(*b*) corresponds to the T-$Al_{78}Mn_{22}$ phase and exhibits a very different shape: the edge has about the same slope as in the I quasicrystal but the intensity at E_F is reduced to 28%. Peak A is split into two subpeaks A′ and A″ at $+1.5 \pm 0.1$ eV and $+2.4 \pm 0.1$ eV, respectively, the FWHM is 3.9 ± 0.1 eV, i.e. considerably narrower than all the other $Al_{100-x}Mn_x$ phases and shoulder S is at the same energy. A similar shape has been obtained from T-$Al_{80}Mn_{20}$ but the curve is broadened especially in the region of shoulder S.

Table 2 summarizes the data corresponding to these different samples.

4. Discussion

Let us recall that, in pure Al, the valence p states extend over about 10 eV and are strongly hybridized with s states over the whole valence band.

$L_{2,3}$ spectra measurements, which provide information on the s valence state distribution, are not available from our samples. Nevertheless, such measurements have been performed by Curry 1968 for crystalline Al_3Mn and by Ederer *et al* (1988) for Al–Mn and Al–Mn–Si alloys. As shown in figure 4, the s state distribution curves of $Al_{100-x}Mn_x$ alloys extend over about the same energy range as those for pure Al, whatever their structural state. The $L_{2,3}$ curve for Al_3Mn shows two wide peaks and is displayed in figure 5 together with our curve for the p state distribution in crystalline $Al_{86}Mn_{14}$. The adjustment in the binding energy scale is made approximately at E_F (within ± 0.2 eV). From the figure, it arises that s states spread widely since they cover about 12 eV. The p states extend over 8 eV, they are mixed with s states but are principally located in the upper part of the valence band. This might be true for all the $Al_{100-x}Mn_x$ alloys.

Our results concerning the Al 3p states show that, although the Mn amount is about 20% atoms, a strong alloying effect is revealed in $Al_{100-x}Mn_x$ mainly through the

Table 2. Structural states of and data on the Al 3p band of our different $Al_{100-x}Mn_x$ alloys.

% Mn atoms	Structural state	FWHM (±0.1 eV)	Peak A energy (±0.1 eV)	Intensity at E_F (±1%)	Splitting of peak A
14	C	4.4	1.65	50	yes
	I	4.5	1.8	42	no
16	C	4.2	1.7	46	yes
	I	4.7	2.0	42	no
20	T	4.1	2.1	32	yes
21	C	4.7	2.0	40	yes
	I	4.3	2.0	34	no
	A	4.2	2.0	28	no
22	T	3.9	2.2	28	yes
pure Al	C	5.3	1.5	50	

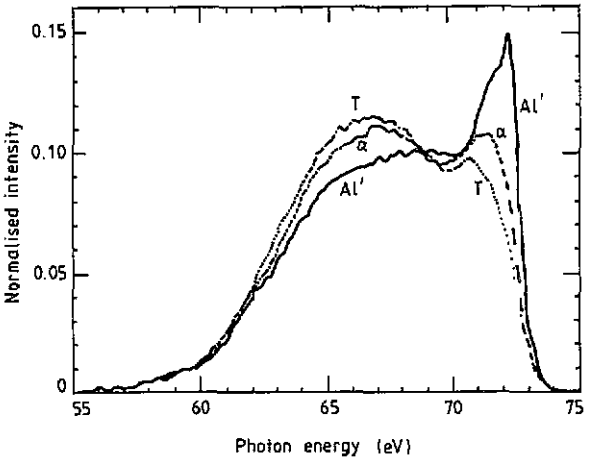

Figure 4. The Al 3s distribution curve of pure Al, C-α AlMnSi and T-AlMn (Ederer *et al* 1988).

narrowing of the Al 3p distribution with respect to pure Al. This is in agreement with the calculations from McHenry *et al* (1986) who have shown that in $MnAl_{12}$ and $MnAl_{32}$ clusters, Mn 3d states hybridize with Al 3p ones to produce a narrowing of the band near E_F. Thus, it is possible to assume that the alloying effect results from the interaction between the rather extended s and p Al states and the more localized d states of the transition metal.

In our samples, the Al 3p distributions are somewhat different according to the structural state. With respect to the metal, we observe a progressive depopulation of the p band near E_F together with a bending of the edge of the distribution and a shift of the maximum A towards a high BE. However, the gravity centre of the band remains roughly unchanged within the experimental accuracy. This leads, when going from crystalline $Al_{86}Mn_{14}$ to I-$Al_{100-x}Mn_x$, T-$Al_{100-x}Mn_x$ and A-$Al_{100-x}Mn_x$, to a decrease of the intensity at E_F. Such a decrease has also been observed by Ederer *et al* (1988) for the s state

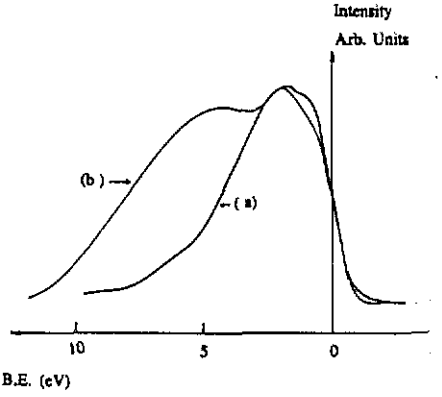

Figure 5. The Al 3p distribution curve in crystalline Al_6Mn, curve (a) and the Al 3s distribution curve in crystalline Al_3Mn, curve (b) (taken from Curry 1968).

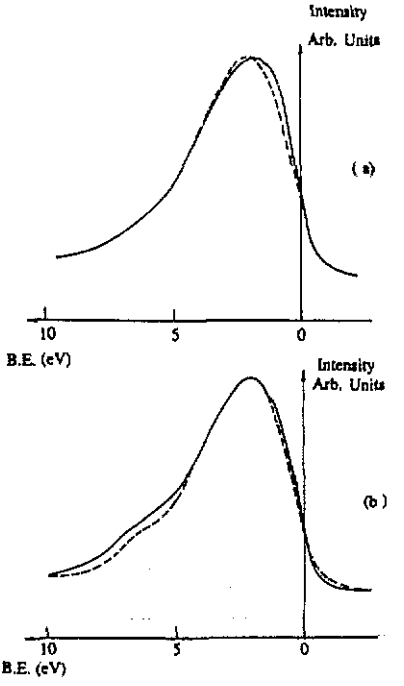

Figure 6. Al 3p distribution curves in two two-phased 'amorphous $Al_{100-x}Mn_x$' samples. Curves (a): full curve, $Al_{84}Mn_{16}$ and broken curve, I-$Al_{84}Mn_{16}$. Curves (b): full curve, $Al_{82}Mn_{18}$ and broken curve, A-$Al_{79}Mn_{21}$.

distribution of several AlMn samples of different nominal compositions from our alloys. Thus, we can conclude that the behaviour of the Al 3p states distribution at E_F reflects that of all of the valence states. Let us note that, from calculations performed in the tight binding method applied to a two-dimensional Penrose lattice, Choy (1985) has predicted an enhancement of the DOS at E_F. This is in contradiction to the experimental results and so this calculation appears not to be suitable for the case of the $Al_{100-x}Mn_x$ quasicrystals. More insight is expected from the study of Al s, d and Mn d state distributions for the alloys used in our experiments.

In table 2 we have reported the relative intensities of our samples measured at E_F. We observe that for a given structural state, when Mn concentration increases in the alloy, the DOS at E_F decreases. All the same, for a given Mn concentration, the DOS at E_F decreases when going from I to T and to A alloys.

The lowering of the DOS at E_F should be reflected in electronic properties such as the resistivity. Several results, available from the literature, are given in table 3.

Resistivity in the quasicrystalline phases is considerably higher (at least one order of magnitude) than in the crystalline counterparts. A and I alloys of the same composition display very similar values, the A phase being more resistive. Resistivity values increasing between the I alloy and the T one with the same Mn content have also been measured (Berger *et al* 1990).

From a general point of view, a decrease in the DOS at E_F can be related to a resistivity increase. Indeed, such a correlation is observed from table 2 column 5 and table 3 column 3 since, for a given structural state, the resistivity increases with the Mn concentration.

Table 3. Resistivity values of different $Al_{100-x}Mn_x$ alloys.

Alloy	Structural state	Resistivity ($\mu\Omega$ cm)	Temperature (K)	Reference
$Al_{86}Mn_{14}$	A	260	30	Nguyen *et al* (1988)
Al_6Mn	C	4.6 80	Low T RT	Dunlap *et al* (1974)
$Al_{86}Mn_{14}$	I C	120 60	300	Lalla *et al* (1987)
$Al_{83}Mn_{17}$	I A	300 400	4.2	Traverse *et al* (1985) Karpe *et al* (1987)
$Al_{80}Mn_{20}$	T	420	300	Berger *et al* (1990)
$Al_{78}Mn_{22}$	T	430	300	Berger *et al* (1990)
$Al_{11}Mn_4$	C	2000		Dunlap *et al* (1976)

As Al_3Mn has been assumed to be a semiconductor (Kolomoets and Popova 1960), the DOS decrease at E_F may be seen as a gap opening correlated to the Mn concentration. This interpretation is supported by our present experimental results. It is also in line with our observations concerning empty Al p DOS (Belin *et al* 1991) from which the edge of the conduction band is repelled progressively from C to I, T and A phases. Indeed, at E_F, the edge of the unoccupied band behaves like that of the emission band. Thus, at half maximum, the distance between the valence and conduction edges increases when passing from C to I, T and A-$Al_{100-x}Mn_x$ alloys.

In crystalline Al_6Mn, whatever the preparation technique, the maximum A of the Al 3p state distribution displays the split shape with the separation at about +1.5 eV, as shown in figure 1. The same is true for α-AlMnSi. This splitting of the Al Kβ band is observed, in the same energy range, for T-AlMn having either 20 or 22% Mn atoms (see figure 3) and is even more marked here than in crystalline Al_6Mn due to the contrast increase which results from the depopulation of states near E_F. Let us recall that in the T-phases of quasicrystalline $Al_{100-x}Mn_x$ structures, along the ten-fold axis, a long-range order symmetry direction is present (Bendersky 1985). In contrast, such behaviour of the Al Kβ band is not observed in either I-$Al_{100-x}Mn_x$ or in A-$Al_{100-x}Mn_x$ alloys in which no long-range structural order exists.

These observations provide evidence that in the $Al_{100-x}Mn_x$ alloys, sp states situated between E_F and the maximum A are very sensitive to modifications of the long range order. So, as previously suggested (Traverse *et al* 1988), we attribute the splitting of the Al 3p states distribution maximum to the presence of a long-range periodicity.

We have used this property to ascertain whether samples were single phased or might contain a crystalline contamination. As an example, we display, in figures 6(*a*) and 6(*b*), the curves obtained from two different samples containing 16 and 18% Mn atoms, respectively, both supposed amorphous since their electron diffraction pattern displayed diffuse halos, but suspected to contain a faint quantity of a crystalline phase. Curves from single phased I-$Al_{84}Mn_{16}$ and A-$Al_{79}Mn_{21}$ are also plotted for comparison. As a matter of fact, from the shape of curve 6(*a*) in particular, we deduced that the sample was micro quasicrystalline and contaminated by a crystalline phase. In the second sample (Mn 18%), which is actually amorphous, the inferring crystalline phase made a very faint

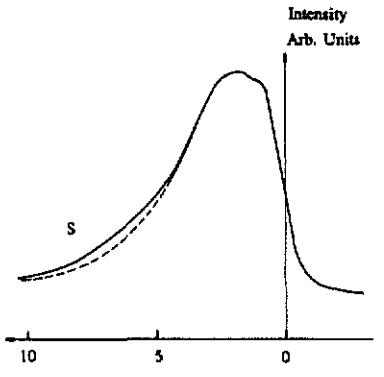

Figure 7. The Al 3p distribution curve in two different crystalline Al_6Mn alloys prepared by the ion beam mixing technique at 500 K (full curve) and at 680 K (broken curve).

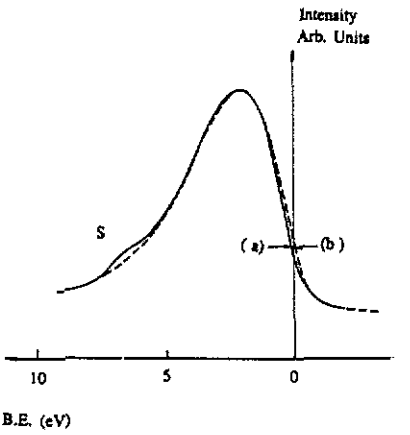

Figure 8. Al 3p distribution curves of the $Al_{79}Mn_{21}$ alloy: (a) A, full curve and (b) I broken curve.

contribution. Let us note that in the curves of figure 6(*b*), features S differ considerably in intensity. We will discuss this point in the next paragraph.

Figure 7 displays the curves obtained from two crystalline Al_6Mn samples prepared by ion beam mixing of Al/Mn multilayers: one is irradiated at 500 K and the other at 680 K. The two curves are identical except in the range of feature S (higher than +4 eV) where they differ noticeably.

As the samples are crystalline, the long-range order is preserved and the local order, depending on first-neighbour distances, is approximately the same as a result of the chemical bonding between Al and Mn. Nevertheless, from one sample to another, crystallographic defects such as dislocations, vacancies, distortions, grain boundaries, etc can be different. Moreover, let us note that the grain size of these samples is very small (50 to 100 Å) and is strongly dependent on the preparation temperature. Consequently, in various samples, differences may arise in a range order short but higher than that of the first neighbours. We will denote short range order by SRO in the following.

Modifications of the high binding energy tail have also been observed from all the other $Al_{100-x}Mn_x$ alloys which we have analysed: I or T as well as A (see figure 6(*b*)). Let us note that in the quasicrystalline alloys, structural defects such as phasons are found which can affect the quasicrystalline state from one sample to another (Kléman 1988).

On the other hand, we have pointed out that the states of the valence band in $Al_{100-x}Mn_x$ alloys are sp hybridized and that from +4 to +12 eV they should be s dominant in character. As the s states are relatively extended states, they can be influenced by changes in the topology of different samples in a range smaller than long range one. Then our results suggest that the states of the valence band of binding energy higher than +4 eV are sensitive to modifications occurring in the SRO so that the higher the intensity of the p states distribution in the energy range of feature S, the more the SRO must be perturbed.

Two samples of about the same composition (20% Mn atoms), prepared by different experimental methods, one being I and the other A, have been considered (figure 8). One expects stronger disorder to be present in the A sample. From the comparison of

the Al 3p bands, it appears that structure S is slightly more intense in A-$Al_{80}Mn_{20}$ than in I-$Al_{80}Mn_{20}$. The respective FWHM and position of maximum A are the same within experimental accuracy. So we suggest that the topological arrangement is the same in the two materials with, indeed, less SRO in the amorphous phase. Further investigations from samples prepared by the same method and with a greater range of compositions are needed to ascertain this point. Let us notice that in amorphous Ni–P alloys with about 20% P atoms, P sp states of the valence band, situated near E_F, have been found to be sensitive to modifications over the range 2 to 4 interatomic distances (Belin *et al* 1987).

We would also like to mention that, contrary to in the case of the other $Al_{100-x}Mn_x$ alloys, in crystalline AlMnSi, the FWHM is higher than in the I counterpart (see table 2) and the whole curve is rather wide. One possible explanation could be that the presence of Si induces disorder in the crystalline phase.

5. Conclusion

We report on an investigation of Al p valence DOS of $Al_{100-x}Mn_x$ alloys with Mn concentrations between 14 and 22% and with various structural arrangements where atomic order is found in different spatial ranges.

It is known that SXS reveals differences in the atomic structure of solids and is, in particular, sensitive to variations in short and medium range order as already observed for amorphous metals and semiconductors with respect to their crystalline counterparts. From our study it results that SXS is also useful in the analysis of quasicrystalline materials since differences are seen in the DOS distributions of I and T phases as well as in A and C ones.

We have pointed out that:

(i) in $Al_{100-x}Mn_x$ alloys, whatever the structural arrangement, due to the alloying effect, the Al 3p distribution is contracted at half maximum with respect to the pure Al;

(ii) the states between E_F and $E_F + 1.5$ eV appear to be very sensitive to modifications in the long-range arrangement, whereas those of binding energy higher than +4.0 eV could be affected by changes in short-range order;

(iii) for a given Mn composition, the DOS at E_F decreases when going from C to quasicrystalline and A alloys;

(iv) for a given structural arrangement, the DOS at E_F decreases when Mn concentration increases.

All our results, together with data obtained by other authors from resistivity measurements, suggest that in $Al_{100-x}Mn_x$ alloys there is a continuous evolution from the metallic state behaviour to the semiconductor behaviour when increasing Mn content, whatever the atomic structure.

Acknowledgments

C Berger (1), J M Dubois (2) and M Harmelin (3) are warmly acknowledged for kindly providing us with as-rapid solidified $Al_{100-x}Mn_x$ samples of different structural states, and for stimulating discussions.

References

Bahadur D, Gaskell P H and Imeson D 1987 *Phys. Lett.* **120A** 417
Belin E, Sénémaud C and Szasz A 1988 *Phil. Mag.* B **58** 551
Belin E, Traverse A and Sadoc A 1991 to be published
Belin E, Traverse A, Szasz A and Machizaud F 1987 *J. Phys. F: Met. Phys.* **17** 1913
Bellissent R, Hippert F, Monod P and Vigneron C 1987 *Phys. Rev.* B **36** 5540
Bendersky L 1985 *Phys. Rev. Lett.* **55** 1461
Bendersky L, Cahn J W and Gratias D 1989 *Phil. Mag.* B **60** 837
Berger C, Gozlan A, Lasjaunias J C, Fourcaudot G and Cyrot-Lackmann F 1990 *Phys. Scr.* at press
Berger C, Pavuna D and Cyrot-Lackmann F 1986 *J. Physique Coll.* 7 C3 489
de Boissieu M, Janot C and Dubois J M 1990 *J. Phys: Condens. Matter* 2 2499
Choy T C 1985 *Phys. Rev. Lett.* **55** 2915
Curry C 1968 *Soft X-ray Band Spectra* ed D J Fabian (New York: Academic) p 173
Denoyer F, Heger G, Lambert M, Audier M and Guyot P 1990 *J. Physique* **51** 651
Dunlap J B, Grünner G and Caplin A D 1974 *J. Phys. F: Met. Phys.* **4** 2203
—— 1976 *Solid State Commun.* **18** 827
Ederer D L, Schaefer R, Tsang K L, Zhang C H, Callcott T A and Arakawa E T 1988 *Phys. Rev.* B **37** 8594
Friedel J 1988 *Helv. Phys. Acta* **61** 538
Fujiwara T 1989 *Phys. Rev.* B **40** 942
Gratias D 1989 *Phys. Scr.* T **29** 38
Guita S, Belin E, Sénémaud C, Udron D, Gheorghiu A and Thèye M L 1986 *J. Physique Coll.* **2** C8 427
Harmelin M 1988 *Quasicrystalline Materials (ILL/CODEST Workshop)* ed C Janot and J M Dubois (Singapore: World Scientific) p 19 and references therein
Ingersent K and Steinhart P J 1990 *Phys. Rev. Lett.* **64** 2034
Karpe N, Rao K V, Bottiger J and Torp B 1987 *Europhys. Lett.* **4** 323
Kléman M 1988 *Quasicrystalline Materials (ILL/CODEST Workshop)* ed C Janot and J M Dubois (Singapore: World Scientific) p 318
Kléman M 1990 *Adv. Phys.* **38** 605
Kolomoets N V and Popova E A 1960 *Fysika Tverdogo Tela* 2 1951
Lalla N P, Singh A K, Stiwari R and Srivastawa N O 1987 *Solid State Commun.* **64** 1409
Mayou D, Maret M and Pasturel A 1988 *Quasicrystalline Materials (ILL/CODEST Workshop)* ed C Janot and J M Dubois (Singapore: World Scientific) p 409
McHenry M E, Eberhart M E, O'Handley R C and Johnson K H 1986 *Phys. Rev. Lett.* **56** 81
Nguyen Van V, Fisson S and Harmelin M 1988 *Mater. Sci. Eng.* **99** 219
Proceedings of the LAM7 Conference 1990 *J. Non-Cryst. Solids* **117, 118**
Sadoc A and Dubois J M 1989 *J. Phys.: Condens Matter* **1** 4283
Sénémaud C 1966 *J. Physique Coll.* **2** C27 55
Shechtman D 1988 *Quasicrystalline Materials (ILL/CODEST Workshop)* ed C Janot and J M Dubois (Singapore: World Scientific) p 3 and references therein
Shechtman D, Blech I, Gratias D and Cahn J W 1984 *Phys. Rev. Lett.* **53** 1951
Smith A P and Ashcroft N W 1987 *Phys. Rev. Lett.* **59** 1365
Traverse A, Dumoulin L, Belin E 1985 *2ème Coll. Nat. sur les Quasicristaux (Rouen, 1985)*
Traverse A, Dumoulin L, Belin E and Sénémaud C 1988 *Quasicrystalline Materials (ILL/CODEST Workshop)* ed C Janot and J M Dubois (Singapore: World Scientific) p 399